Ground-state candidate for the classical dipolar kagome Ising antiferromagnet

I. A. Chioar, N. Rougemaille, and B. Canals
CNRS, Institut NÉEL, F-38000 Grenoble, France
and Université Grenoble Alpes, Institut NÉEL, F-38000 Grenoble, France
(Received 3 December 2015; revised manuscript received 16 May 2016; published 9 June 2016)

We have investigated the low-temperature thermodynamic properties of the classical dipolar kagome Ising antiferromagnet using Monte Carlo simulations, in the quest for the ground-state manifold. In spite of the limitations of a single-spin-flip approach, we managed to identify certain ordering patterns in the low-temperature regime and we propose a candidate for this unknown state. This configuration presents some intriguing features and is fully compatible with the extrapolations of the at-equilibrium thermodynamic behavior sampled so far, making it a very likely choice for the dipolar long-range ordered state of the classical kagome Ising antiferromagnet.

DOI: 10.1103/PhysRevB.93.214410

I. INTRODUCTION

Dipolar long-range interactions can often lead to unconventional arrangements of magnetic moments, particularly when their interplay with the spatial distribution of these moments gives rise to frustration. One typical example can be found in spin ice pyrochlores, such as $Ho_2Ti_2O_7$ [1] and $Dy_2Ti_2O_7$ [2], where the observed icelike physics has a deep dipolar root [3]. Artificial realizations that mimic the frustration-induced effects encountered in such condensed matter compounds have recently attracted much interest and have generally taken the form of lithographically patterned arrays of magnetic nanoislands, bearing the name of artificial spin ices [4,5]. The magnetostatic framework of these arrays, the almost infinite freedom in design, and the possibility to locally probe each magnetic component have enabled the exploration of a wide range of intriguing phenomena over the past few years [6,7].

Several artificial frustrated systems have been studied, with a particular attention given to square and kagome geometries with in-plane magnetized elements. Nevertheless, another type of kagome network has been recently fabricated [8,9], with magnetic moments pointing perpendicular to the lattice plane. This so-called kagome Ising system presents only antiferromagnetic pairwise couplings, contrary to its in-plane counterpart, the kagome spin ice, which displays a mixture of ferro- and antiferromagnetic interactions, depending on the relative orientation of the considered pair of spins (see Fig. 1). If governed solely by nearest-neighbor spin couplings, these two kagome spin networks show identical thermodynamic behavior. More specifically, they both present a crossover from the paramagnetic phase into a spin ice manifold, where each triangle respects the so-called kagome ice rules, requiring the existence of a minority spin per triangle. This local constraint minimizes nearest-neighbor interactions and, within this short-range interaction picture, yields a macroscopically degenerated ground-state manifold [10,11] characterized by a cooperative paramagnetic regime [12] and exponentially decaying pairwise spin correlations. However, dipolar long-range contributions lift this degeneracy and determine distinctive low-temperature behavior for the two kagome networks, each of them having its own story to tell [9]. Otherwise said, the longer range couplings enrich the palette of unconventional magnetic phases that can potentially be achieved within the framework of artificial spin ices and a simple change in the spin orientation can yield completely new spin textures, even when the lattice topology is preserved. However, while the thermodynamic features of kagome spin ice have been thoroughly investigated numerically [13,14] and its phase space has been intensively explored experimentally [15–22], the low-temperature properties of the dipolar kagome Ising antiferromagnet remain mostly unaddressed, both theoretically and experimentally, and a main challenge is to study the potential formation of long-range spin order.

By employing Monte Carlo simulations, we have explored the at-equilibrium thermodynamic features of this spin model, particularly in the low-temperature regime. Although our Metropolis Monte Carlo approach [23] does not manage to simulate the full recovery of the magnetic degrees of freedom, we believe that this system ultimately achieves long-range spin order and we provide a candidate for its dipolar long-range ground state. Some studies have been previously performed on the kagome Ising antiferromagnet considering first, second, and even third order spin couplings [24–27], but, to the best of our knowledge, this state has not been reported before. Furthermore, it also proves to be fully compatible with the thermodynamic features sampled so far, making it a very likely choice for the lowest-energy state of the dipolar kagome Ising antiferromagnet.

In addition to the description based on the spin degrees of freedom, we have also employed the magnetic charge picture, which generally consists of replacing each spin with a pair of opposite, classical magnetic charges [28]. For the case of kagome spin ice, all spins lie in the network's plane and, since each spin is the connection point between two neighboring kagome triangles, it contributes with a positive unitary magnetic charge in one triangle and a negative unitary magnetic charge in the other. Furthermore, individual charge contributions coming from any three spins that share the same kagome triangle can be summed up at the vertex sites, thus ultimately yielding an effective hexagonal array of vertex magnetic charges. Since the Ising spins can be written as the product between a ± 1 scalar value (σ_u) and a vector ($\vec{e}_u$) that defines the spin direction along the bisectors of a kagome triangle, $\vec{S}_u = \sigma_u \cdot \vec{e}_u$, the values of each vertex charge can be expressed as a sum of the Ising states of the spins located at the corners of its corresponding triangle:

$$Q_\Delta = \sum_{u\in\Delta} \sigma_u, \quad Q_\nabla = -\sum_{u\in\nabla} \sigma_u, \tag{1}$$

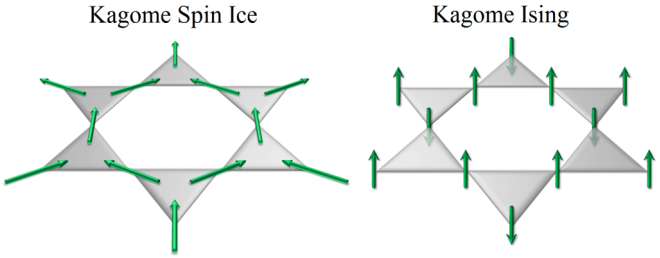

FIG. 1. The kagome lattice is a triangular network of corner-sharing triangles. Two particular arrays have been fabricated so far in the framework of artificial spin ice: the kagome spin ice, with the Ising-like spins lying in the network plane, and the kagome Ising, with spins pointing along the vertical axis.

where Q_Δ and Q_∇ represent the charge values for a Δ-shaped and ∇-shaped triangle, respectively, and the minus sign in the latter expression ensures global charge neutrality. Although less intuitive, vertex charge states can also be defined for the kagome Ising network as well by following this convention (in that case, $\vec{e}_u = \vec{e}_z$ for every lattice site).

This effective charge description has proven to be particularly useful in the case of dipolar kagome spin ice, which presents a two-stage ordering process [13,14], passing through a so-called spin ice 2 phase before achieving long-range spin order. This intermediate state is characterized by the coexistence of spin order and disorder [29,30] and is also regarded as an algebraic spin liquid that sits upon an emergent magnetic charge crystal [13,14]. Furthermore, this charge framework has been successfully employed to experimentally highlight the differences in the behavior of the two dipolar kagome networks [9,17].

The remainder of this paper is organized into four main sections. We shall first present the model employed along with the parameters of our Monte Carlo simulations. Afterwards, the candidate state will be described using both the spin and effective magnetic charge pictures. A specific section is then dedicated to the properties of this ground-state candidate and its compatibility with the at-equilibrium thermodynamics sampled so far. Furthermore, a discussion will follow, focusing on some of the intriguing features that this state displays. Lastly, conclusions are provided along with potential routes for future investigations.

II. THE MODEL AND THE SIMULATIONS

We have performed Monte Carlo simulations for kagome Ising networks with $L \times L \times 3$ lattice sites (L ranging from 12 to 36) using the dipolar spin ice Hamiltonian [3]. Given the Ising nature of the spins and the fact that they all share the same quantization axis ($\vec{e}_z$), the Hamiltonian can be brought to a more compact, scalar form:

$$H = J_0 \sum_{\langle u<v \rangle} \sigma_u \sigma_v + D \sum_{(u<v)} \frac{\sigma_u \sigma_v}{r_{uv}^3}, \qquad (2)$$

where σ_u and σ_v represent the Ising states ($\vec{S}_u = \sigma_u \cdot \vec{e}_z$ and $\sigma_u = \pm 1$), r_{uv} stands for their relative position, D is the dipolar constant, and J_0 is an additional coupling that corrects the interaction between nearest neighbors, should it deviate from the dipolar approximation. More specifically, in the case of artificial spin ices, the finite size of the elements can slightly alter the Ising nature of the nanoislands, while proximity effects can result in deviations from the point-dipole approximation. Nevertheless, using micromagnetic simulations, these effects have been reported to significantly affect only nearest-neighbor couplings, and can actually be accounted for by the addition of a nearest-neighbor exchange-like term [17]. Following a similar approach, we noticed that there is only a slight deviation for nearest neighbors in the case of our previously studied artificial kagome Ising samples [9], yielding $J_0 \cong (1/2)D_{\text{eff}}$, where $D_{\text{eff}} = D/r_{NN}^3$. This allows us to define the effective nearest-neighbor coupling as $J_{NN} = J_0 + D/r_{NN}^3 = (3/2)(D/r_{NN}^3)$. Periodic boundary conditions have been implemented and the pairwise couplings are summed up within a maximum radius disk such that a spin does not interact with one of its images [31]. Starting from a paramagnetic regime ($T/J_{NN} = 100$), the temperature is gradually dropped down. A Metropolis single-spin-flip algorithm has been employed and, for each temperature value, we used 10^4 modified Monte Carlo steps (MMCS) for thermalization followed by 10^4 MMCS for sampling decorrelated spin configurations and computing relevant thermodynamic quantities (see note [32] for more details on MMCS).

After the system reaches the spin ice phase and all triangles respect the kagome ice rule, longer range contributions further correlate the system. The single-spin-flip dynamics still manages to ergodically map the phase space down to a deep spin ice temperature, but it ultimately suffers from a critical slowing down effect for $T/J_{NN} \cong 0.03$, at a point where the system seems to be experiencing a phase transition. A similar phenomenon occurs for dipolar kagome spin ice at the onset of the spin ice 2 phase, but this algorithmic inconvenience can be overcome by including collective spin flips [33] in the form of closed spin loops [13,14,34]. These loop updates ensure that the kagome ice rules are not violated while they also preserve an already-established antiferromagnetic charge order. The former argument has motivated us to apply this collective spin dynamics to the kagome Ising system as well, where the loops become alternating, closed chains of spins. While this addition enhances the exploration of the warm spin ice regime, these collective spin flips are increasingly rejected at lower temperatures and this particular dynamics ultimately freezes at roughly the same point as the single spin flips do. Nevertheless, the thermodynamic behavior sampled so far proves to be useful and, with the help of a geometrical construction, ordering tendencies can be revealed, in direct space, at the lowest temperatures. These have ultimately led us to the ground-state candidate that we propose, a configuration to which we shall refer to as the 7-shaped phase.

III. THE GROUND-STATE CANDIDATE

Our candidate is a rectangular crystal of a 12-spin magnetic unit cell, commensurable with the underlying triangular Bravais lattice, as reproduced in Fig. 2(a). Although there are many different ways in which the 12-spin magnetic unit cell can be defined, we have opted here for the one revealed by the so-called *arrow picture*, which consists of drawing an arrow from all spin-up states to all their nearest-neighboring spin-down

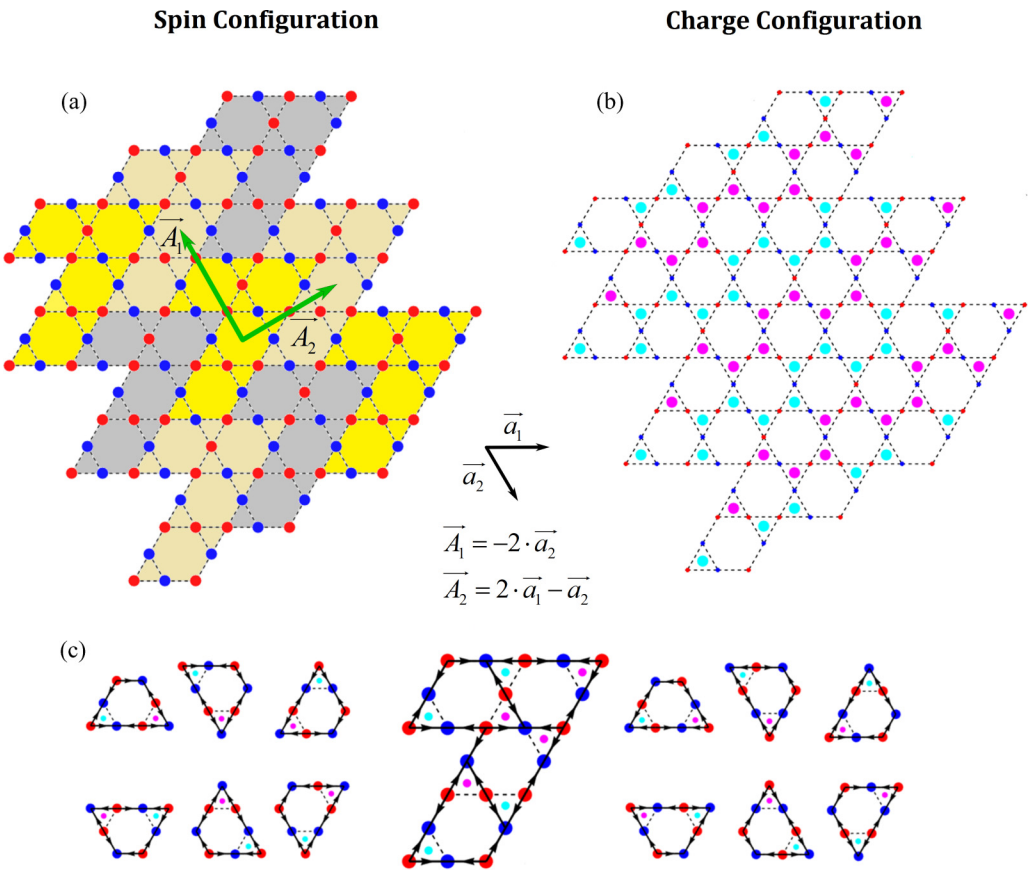

FIG. 2. The 7-shaped phase—a candidate for the ground state of the dipolar kagome Ising network. (a) The spin configuration is a crystal of 7-shaped unit cells with a rectangular basis $(\vec{A}_1,\vec{A}_2)$, which can be made commensurable with the Bravais triangular basis $(\vec{a}_1,\vec{a}_2)$ of the original kagome network. Each unit cell contains (a) 12 spins, represented here by red and blue dots corresponding to the up and down states respectively, and (b) 8 vertex magnetic charges, represented by magenta and cyan dots for the $+1$ and -1 states, respectively. (c) The arrow picture representation for this configuration reveals the 7-shaped unit cells, which are in turn made out of alternating sequences of spins that define the perimeters of trapezoidal shapes with different orientations.

states. This geometrical construction maps the local stray field lines between nearest-neighboring spins in a magnetostatic framework and can highlight magnetic moment organizations that are energetically favorable locally. By applying it to configurations sampled by our Monte Carlo simulations in the low-temperature regime of the dipolar kagome Ising antiferromagnet, a tessellation of trapezoidal shapes can be revealed, where each trapezoid's perimeter is a chain of alternating up and down nearest-neighboring spin states [see Fig. 2(c)]. The 7-shaped unit cells are then formed by an appropriate organization of four such trapezoidal shapes. Given the rotational and time-reversal symmetries of these 7-shaped unit cells, the candidate configuration is sixfold degenerated.

If we now consider the effective magnetic charge description, each unit cell contains 8 vertex magnetic charges, as can be seen in Fig. 2(b). However, there is an equal amount of positive and negative unitary charges per unit cell, thus making the latter charge neutral. On a network scale, these charges ultimately organize into an alternating sequence of positively and negatively charged zigzag-like stripes [see Fig. 2(b)], which are, in fact, aligned with one of the rectangular crystal vectors, while alternating in sign along the other. This is in sharp contrast with the antiferromagnetic charge order specific to the low-temperature regime of dipolar kagome spin ice and actually indicates a preference for a ferromagnetic charge arrangement.

With the spin and charge descriptions of this candidate state at hand, we will now turn to verifying its viability as a ground-state configuration. This can be primarily done by checking its compatibility with the thermodynamic behavior sampled so far.

IV. COMPATIBILITY OF THE 7-SHAPED PHASE

First, for this candidate to truly be a ground state, its energy has to be the lowest possible within the dipolar framework. In fact, the energy/spin of this configuration is $e/J_{NN} = -0.6744$ and it is lower than all the other values sampled throughout the entire simulation [see Fig. 3(a)]. Notice the relatively small difference between this value and the energy of the ground state of a kagome Ising antiferromagnet governed only by nearest-neighbor couplings, which, for the current parameters, would be $e_{SR}/J_{NN} = -2/3$. While this slight difference might conceal the importance of longer range coupling terms, their impact is highlighted by the temperature evolutions of the network averages of the pairwise spin correlators, $C_{\alpha j}(T) = \langle \sigma_\alpha \sigma_j \rangle (T)$, which can also serve as test

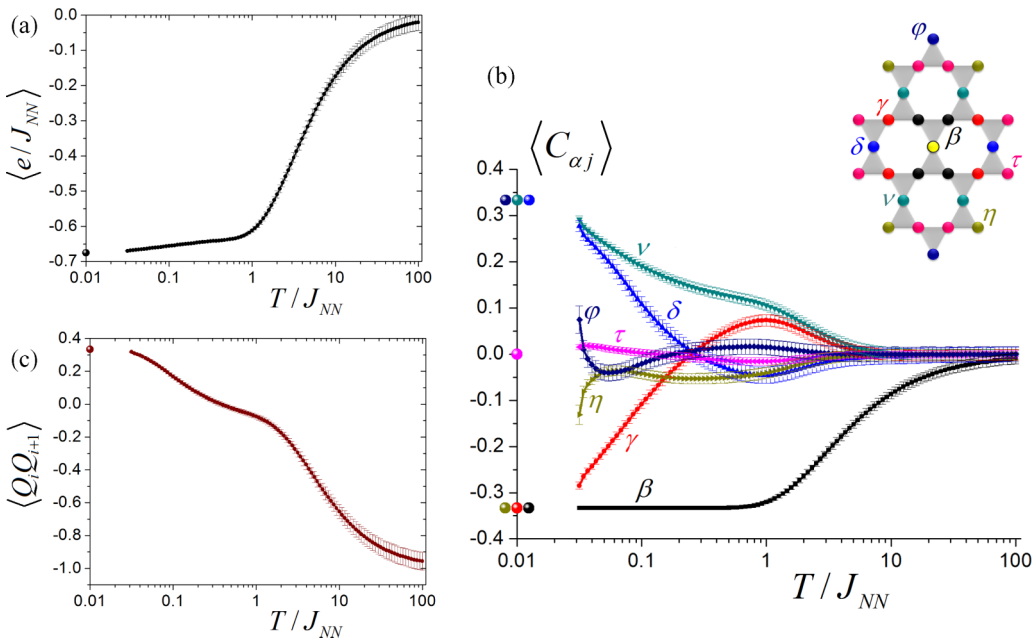

FIG. 3. The temperature dependencies of the average values of different thermodynamic quantities computed for a dipolar kagome Ising network with $36 \times 36 \times 3$ lattice sites within the simulated temperature window, prior to the critical slowing down of the single-spin-flip dynamics. In all three cases, the error bars correspond to the standard deviation of the distribution of values sampled for each Monte Carlo temperature and the colored dots highlight the values extracted from the candidate state. (a) After minimizing nearest-neighbor interactions, the average energy continues to decrease steadily, reaching a value of $\langle e_{LT}/J_{NN}\rangle = -0.6702$ for the lowest simulated temperature, slightly higher than the 7-shaped phase one, $e_{7B}/J_{NN} = -0.6744$. (b) The evolution of the first seven pairwise spin correlators, as defined in the inset. All plots aim for the values computed from the 7-shaped phase, thus reflecting the system's apparent desire to reach it. With the exception of $C_{\alpha\tau}$, all values tend to $\pm 1/3$. In fact, the $\alpha\beta$,$\alpha\gamma$, and $\alpha\eta$ pairs form kagome networks that fully respect the kagome ice rule. (c) The nearest-neighbor charge correlator displays a monotonic behavior, continuously increasing and apparently aiming for the value of $+1/3$, compatible once again with the proposed configuration.

agents for the compatibility of the 7-shaped state with the sampled thermodynamic behavior.

The development of the first seven pairwise spin correlators, as defined by Wills *et al.* [27], is given in Fig. 3(b), along with the values extracted from our ground-state candidate. Notice how the latter play the role of target values for the evolution of the former, thus emphasizing the compatibility of the 7-shaped state with the extrapolations of the behavior sampled so far. The same feature can be observed if the charge description is now considered and the nearest-neighbor charge correlator, $Q_i Q_{i+1}$, is computed. As previously reported [9], the kagome Ising charge correlator becomes positive deep within the spin ice phase and appears to evolve towards the value of $+1/3$ [see Fig. 3(c)]. This would imply that, on average, each vertex charge is surrounded by two nearest neighbors of the same sign and one with the opposite. This is exactly the case in the 7-shaped phase, where each local charge correlator is equal to $+1/3$, given the formation of winding charged stripes.

In addition, snapshots sampled in heat-bath conditions at low temperatures contain patches of the candidate configuration. In fact, the arrow picture unveils a tessellation of trapezoidal shapes which seem to struggle to align with the already-established 7-shaped clusters. The presence and distribution of these domains can be quantified for each temperature by computing the spin structure factor, i.e., the Fourier transform of the spin correlation function:

$$S(\vec{k}) = \sum_{(u,v)} \langle \sigma_u \sigma_v \rangle \exp[-i \vec{r}_{uv} \vec{k}], \tag{3}$$

where σ_u and σ_v stand for lattice Ising spins, r_{uv} is their relative position in direct space, and $\vec{k}$ is a vector of the reciprocal space.

Figure 4 presents the temperature plots of the specific heat and the entropy of the dipolar kagome Ising network along with typical spin structure factor maps for each regime. As the system cools and the spins correlate, the diffuse background of the structure factor gradually disappears and Bragg peaks start to develop around certain Γ and M points. In addition, there are some faint peaks forming along the Γ-K lines, at 3/4 of the distance from the center of the Brillouin zones. In fact, this entire behavior is compatible with the 7-shaped phase (see the maps of Fig. 4). Its spin structure factor selectively displays Bragg peaks for certain Γ and M points, as well as along some Γ-K lines, at 3/4 of the distance. These features can be somewhat easily understood by referring to the magnetic charge stripe organization. These stripes repeat themselves every two lattice parameters along the $\vec{a}_2$ direction and, along a stripe's direction, display a zigzag periodicity defined by $\vec{A}_1$, a typical Γ-K vector (see Fig. 2). However, given the sixfold degeneracy, all possible domain orientations are present at the last-sampling temperature and the structure factor map is a linear

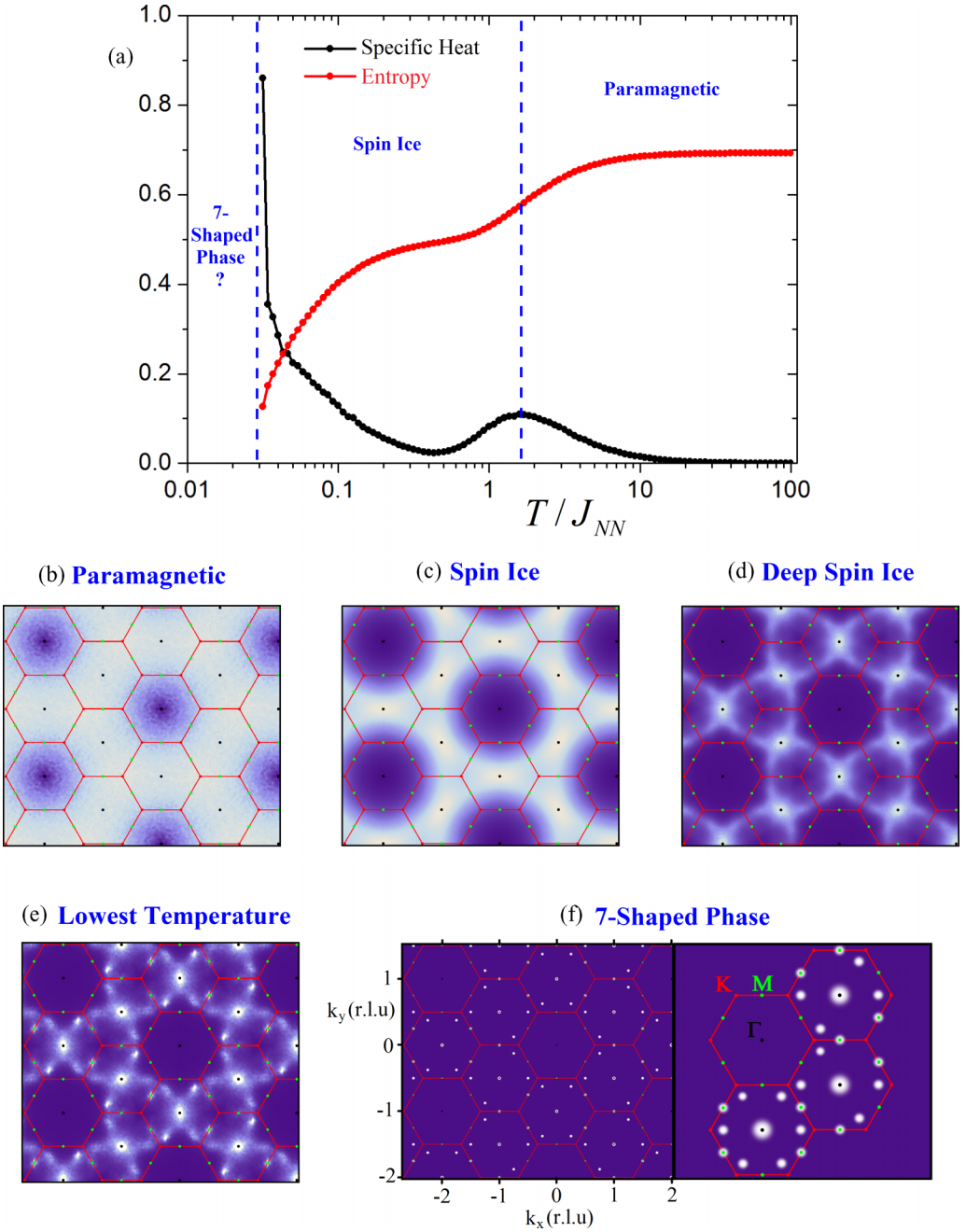

FIG. 4. (a) The specific heat and the entropy of a dipolar kagome Ising antiferromagnet with $36 \times 36 \times 3$ lattice sites, as sampled by a single-spin-flip dynamics. The sharp increase in the specific heat signals the presence of an apparent phase transition at $T/J_{NN} \cong 0.03$, deep within the spin ice phase. (b)–(e) Typical spin structure factor maps are given for each temperature regime and show how the system evolves towards (f) the sixfold-averaged map of the 7-shaped phase, a reconstruction of which is provided separately for more clarity. Notice how the map of the last sampling temperature still displays a diffuse kagome-like structure, typical of a deep spin ice regime, but starts building up the Bragg peaks specific to the 7-shaped phase. This is due to the presence of relatively large clusters of the candidate configuration at this stage.

combination of the three possibilities. This suggests, yet again, the compatibility of the candidate ground state with the ordering tendencies of the dipolar kagome Ising antiferromagnet.

V. DISCUSSION

Although these examples are necessary but not sufficient conditions for confirming the validity of this configuration as the long-range dipolar ground state, the 7-shaped phase has proven to be fully compatible with the extrapolations of all thermodynamic quantities sampled so far, thus making it a very likely candidate. Interestingly, it displays a 6-fold degeneracy, similar to the ground states of other kagome-based dipolar spin models [35,36].

As previously mentioned, the 12-spin magnetic unit cell can be defined in different ways, but the trapezoidal formations revealed by the arrow picture may prove useful for unraveling an appropriate spin dynamics that can potentially overcome

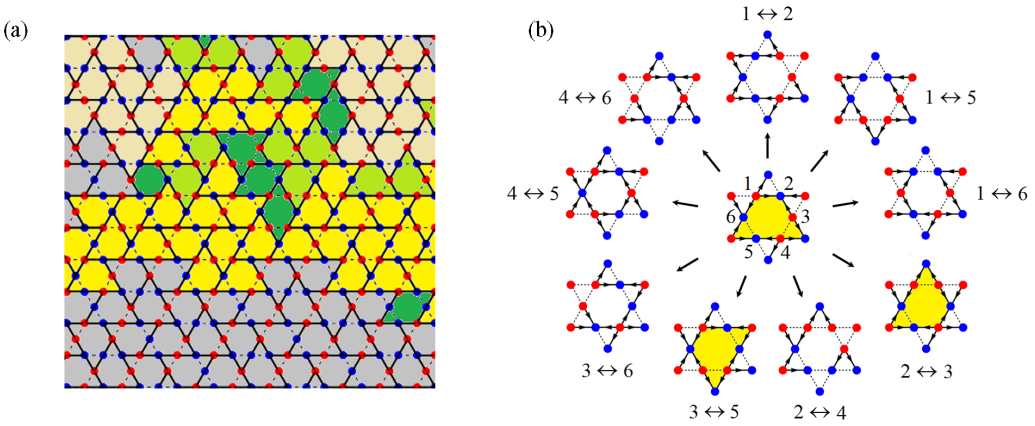

FIG. 5. (a) A low-temperature snapshot ($T/J_{NN} \cong 0.03$) from a region of a $36 \times 36 \times 3$ dipolar kagome Ising network showing the formation of 7-shaped domains with different orientation axes (gray, yellow, and faded yellow areas). The green areas are trapezoids that do not fit within any of the clusters, while the dark green areas mark defects that do not form preferential trapezoidal structures. Expanding the clusters or adjusting one to fit a neighbor is clearly beyond the practical use of the single-spin-flip dynamics. However, by interchanging a pair of opposite spins from its inner hexagon (b), the trapezoid's orientation can be modified. Notice that, in this example, only two out of the nine possible scenarios can preserve the initial shape, forming potentially favorable configurations, while other choices can even result in the creation of kagome-ice-rule-breaking triangles. Therefore, selectively choosing the spin pairs and extending the procedure over larger areas can potentially result in an efficient cluster dynamics that can enhance the exploration of these low-energy manifolds.

the critical slowing down of single spin flips, which are rather inefficient for expanding or merging already-formed 7-shaped clusters. By flipping certain pairs of up and down spins within the internal hexagon of a trapezoidal formation, the trapezoid's orientation can be changed (see Fig. 5), potentially adjusting it to its environment. However, it is worth noting that one such update can also lead to the creation of defects or even ice-rule-breaking configurations, which would be immediately rejected by the detailed balance condition. Therefore, this procedure might have to be applied repeatedly over numerous trapezoids or even selectively to several at a time, in the form of a collective spin dynamics [33].

Another interesting feature of the 7-shaped phase, and of the dipolar kagome Ising antiferromagnet in general, is the formation of magnetic charged stripes. These structures, along with the positive values of the nearest-neighbor charge correlator, highlight the preference for a ferromagnetic charge order, in sharp contrast with dipolar kagome spin ice. However, a perfect ferromagnetic charge crystal is impossible to achieve at the network scale due to the requirement for global charge neutrality, thus leaving the magnetostatically favorable option of forming charged lines that effectively screen each other out by alternating. This behavior emphasizes the strong impact that a change in the spin's geometry can have on the organization of the emerging charge field.

VI. CONCLUSION

In conclusion, the development of long-range ordered states in the dipolar kagome Ising antiferromagnet have been studied via Monte Carlo simulations, in the quest for the ground-state configuration. In spite of the algorithmic limitations, we can nevertheless provide a candidate for this unknown state through the use of a geometrical construction based on a phenomenological approach. This so-called 7-shaped phase is a rectangular crystal of a 12-spin magnetic unit cell and has proven to be fully compatible with all thermodynamic features observed so far, making it a very likely choice for the dipolar long-range ground state of the kagome Ising antiferromagnet.

From a numerical point of view, the challenge still remains to find a collective spin dynamics that can properly access this state and even characterize the apparent phase transition. Experimentally, such intriguing spin textures can potentially be achieved within the framework of artificial spin ices, particularly using thermally active structures, which, for certain protocols, can somewhat overcome the intrinsic slowing down of single spin flips and locally retrieve low-energy states that are hardly accessible otherwise [20].

ACKNOWLEDGMENTS

This work was partially supported by the Agence Nationale de la Recherche through Project No. ANR12-BS04-009 "Frustrated." I.A.C. acknowledges financial support from the Laboratoire d'excellence LANEF Grenoble and is grateful to Karim Ferhat for several fruitful discussions.

[1] M. J. Harris, S. T. Bramwell, D. F. McMorrow, T. Zeiske, and K. W. Godfrey, Phys. Rev. Lett. **79**, 2554 (1997).

[2] A. P. Ramirez, A. Hayashi, R. J. Cava, R. Siddharthan, and B. S. Shastry, Nature (London) **399**, 333 (1999).

[3] B. C. den Hertog and M. J. P. Gingras, Phys. Rev. Lett. **84**, 3430 (2000).
[4] R. F. Wang, C. Nisoli, R. S. Freitas, J. Li, W. McConville, B. J. Cooley, M. S. Lund, N. Samarth, C. Leighton, V. H. Crespi, and P. Schiffer, Nature (London) **439**, 303 (2006).
[5] M. Tanaka, E. Saitoh, H. Miyajima, T. Yamaoka, and Y. Iye, Phys. Rev. B **73**, 052411 (2006).
[6] C. Nisoli, R. Moessner, and P. Schiffer, Rev. Mod. Phys. **85**, 1473 (2013).
[7] L. J. Heyderman and R. L. Stamps, J. Phys.: Condens. Matter **25**, 363201 (2013).
[8] S. Zhang, J. Li, I. Gilbert, J. Bartell, M. J. Erickson, Y. Pan, P. E. Lammert, C. Nisoli, K. K. Kohli, R. Misra, V. H. Crespi, N. Samarth, C. Leighton, and P. Schiffer, Phys. Rev. Lett. **109**, 087201 (2012).
[9] I. A. Chioar, N. Rougemaille, A. Grimm, O. Fruchart, E. Wagner, M. Hehn, D. Lacour, F. Montaigne, and B. Canals, Phys. Rev. B **90**, 064411 (2014).
[10] I. Syôzi, Prog. Theor. Phys. **6**, 306 (1951).
[11] K. Kanô and S. Naya, Prog. Theor. Phys. **10**, 158 (1953).
[12] J. Villain, Z. Phys. B **33**, 31 (1979).
[13] G. Möller and R. Moessner, Phys. Rev. B **80**, 140409 (2009).
[14] G.-W. Chern, P. Mellado, and O. Tchernyshyov, Phys. Rev. Lett. **106**, 207202 (2011).
[15] Y. Qi, T. Brintlinger, and J. Cumings, Phys. Rev. B **77**, 094418 (2008).
[16] J. Li, X. Ke, S. Zhang, D. Garand, C. Nisoli, P. Lammert, V. H. Crespi, and P. Schiffer, Phys. Rev. B **81**, 092406 (2010).
[17] N. Rougemaille, F. Montaigne, B. Canals, A. Duluard, D. Lacour, M. Hehn, R. Belkhou, O. Fruchart, S. El Moussaoui, A. Bendounan, and F. Maccherozzi, Phys. Rev. Lett. **106**, 057209 (2011).
[18] S. Zhang, I. Gilbert, C. Nisoli, G.-W. Chern, M. J. Erickson, L. OBrien, C. Leighton, P. E. Lammert, V. H. Crespi, and P. Schiffer, Nature (London) **500**, 553 (2013).
[19] F. Montaigne, D. Lacour, I. A. Chioar, N. Rougemaille, D. Louis, S. M. Murtry, H. Riahi, B. S. Burgos, T. O. Menteş, A. Locatelli, B. Canals, and M. Hehn, Sci. Rep. **4**, 5702 (2014).
[20] I. A. Chioar, B. Canals, D. Lacour, M. Hehn, B. Santos Burgos, T. O. Menteş, A. Locatelli, F. Montaigne, and N. Rougemaille, Phys. Rev. B **90**, 220407 (2014).
[21] J. Drisko, S. Daunheimer, and J. Cumings, Phys. Rev. B **91**, 224406 (2015).
[22] L. Anghinolfi, H. Luetkens, J. Perron, M. G. Flokstra, O. Sendetskyi, A. Suter, T. Prokscha, P. M. Derlet, S. L. Lee, and L. J. Heyderman, Nat. Commun. **6**, 8278 (2015).
[23] N. Metropolis, A. W. Rosenbluth, M. N. Rosenbluth, A. H. Teller, and E. Teller, J. Chem. Phys. **21**, 1087 (1953).
[24] P. Azaria, H. T. Diep, and H. Giacomini, Phys. Rev. Lett. **59**, 1629 (1987).
[25] M. Wolf and K. D. Schotte, J. Phys. A: Math. Gen. **21**, 2195 (1988).
[26] T. Takagi and M. Mekata, J. Phys. Soc. Jpn. **62**, 3943 (1993).
[27] A. S. Wills, R. Ballou, and C. Lacroix, Phys. Rev. B **66**, 144407 (2002).
[28] C. Castelnovo, R. Moessner, and S. L. Sondhi, Nature (London) **451**, 42 (2008).
[29] M. E. Brooks-Bartlett, S. T. Banks, L. D. C. Jaubert, A. Harman-Clarke, and P. C. W. Holdsworth, Phys. Rev. X **4**, 011007 (2014).
[30] B. Canals, I. A. Chioar, V. D. Nguyen, M. Hehn, D. Lacour, F. Montaigne, A. Locatelli, T. O. Menteş, B. Santos Burgos, and N. Rougemaille, Nat. Commun. **7**, 11446 (2016).
[31] Cutting off the summation over the dipolar couplings can severely affect the system's behavior, particularly in the low-temperature regime. However, for two-dimensional lattices, the dipolar summation is absolutely convergent and, if sufficient terms are considered, the overall thermodynamic features are well captured. We have performed Monte Carlo simulations, as described in the main text, for kagome networks with $L \times L \times 3$ sites, where L can be either 12, 18, 21, or 36. The same thermodynamic behavior is found in each case, with a slight variation in the position of the specific heat peak that signals an apparent phase transition deep within the spin ice phase. Nevertheless, the simulation is halted at this stage as the driving spin dynamics can no longer ensure the ergodic exploration of these low-energy manifolds.
[32] While a Monte Carlo step is genuinely considered as a sweep through the entire lattice, it is not necessarily equal to a unit of Monte Carlo time, which would ensure minimal decorrelation between successively sampled configurations. Therefore, several sweeps are performed between consecutively sampled states and the number of intermediate Monte Carlo steps, called a modified Monte Carlo step, is taken as a multiple of the inverse spin acceptance ratio, which in turn is computed during every thermalization stage.
[33] U. Wolff, Phys. Rev. Lett. **62**, 361 (1989).
[34] R. G. Melko, B. C. den Hertog, and M. J. P. Gingras, Phys. Rev. Lett. **87**, 067203 (2001).
[35] M. Maksymenko, V. R. Chandra, and R. Moessner, Phys. Rev. B **91**, 184407 (2015).
[36] M. S. Holden, M. L. Plumer, I. Saika-Voivod, and B. W. Southern, Phys. Rev. B **91**, 224425 (2015).